American Mineralogist, Volume 82, pages 607–619, 1997

Clarkeite: New chemical and structural data

ROBERT J. FINCH* AND RODNEY C. EWING

Department of Earth and Planetary Sciences, University of New Mexico, Albuquerque, New Mexico 87131, U.S.A.

ABSTRACT

Clarkeite crystallizes during metasomatic replacement of pegmatitic uraninite by late-stage, oxidizing hydrothermal fluids. Samples are zoned compositionally: Clarkeite, which is Na rich, surrounds a K-rich core (commonly with remnant uraninite) and is surrounded by more Ca-rich material; volumetrically, clarkeite is most abundant. Clarkeite is hexagonal (space group $R\bar{3}m$) $a = 3.954(4)$, $c = 17.73(1)$ Å ($Z = 3$). The structure of clarkeite is based on anionic sheets of the form $[(UO_2)(O,OH)_2]$. The sheets are bonded to each other through interlayer cations and H_2O molecules. The empirical formula for clarkeite from the Fanny Gouge mine near Spruce Pine, North Carolina, is:

$$\{Na_{0.733}K_{0.029}Ca_{0.021}Sr_{0.009}Y_{0.024}Th_{0.006}Pb_{0.058}\}_{\Sigma 0.880}[(UO_2)_{0.942}O_{0.918}(OH)_{1.082}](H_2O)_{0.069.}$$

Na predominates and the Pb is radiogenic. The general formula for clarkeite is

$$\{(Na,K)_pM^{2+}_qM^{3+}_rM^{4+}_sPb_x\}[(UO_2)_{1-x}O_{1-y}(OH)_{1+y}](H_2O)_z$$

where Na >> K and $p > (q + r + s)$. The number of O^{2-} ions and OH groups in the structural unit is determined by the net charge of the interlayer cations (except Pb): $y = 1 - (p + 2q + 3r + 4s)$. This suggests that the ideal formula for ideal end-member clarkeite is $Na[(UO_2)O(OH)](H_2O)_{0\text{-}1}$. The structural sheets are destabilized as U decays to Pb (increasing x), and Pb enters vacant interlayer cation sites. Clarkeite eventually recrystallizes to lead uranyl oxide hydrates such as wölsendorfite or curite.

INTRODUCTION

Clarkeite is a U^{6+} oxide of variable composition and previously uncertain structure. A large number of U^{6+} minerals are known (Frondel 1958; Smith 1984; Burns et al. 1996). Most U^{6+} minerals are weathering products formed at or near the surface (Frondel 1956; Finch and Ewing 1992), whereas clarkeite forms by oxidation and replacement of uraninite late during pegmatite crystallization (Ross et al. 1931; Finch and Ewing 1993). Although uraninite-bearing granite pegmatites are common, clarkeite is known from only two localities.

Clarkeite is the only known naturally occurring high-temperature uranate. Anhydrous high-temperature uranates have been synthesized from oxide melts above approximately 800 °C (Lindemer et al. 1981; Toussaint and Avogadro 1974); hydrous uranates are precipitated from aqueous solutions above 250 °C (Cordfunke and Loopstra 1971; Kovba et al. 1958) or as low as 25 °C (Wamser et al. 1952). Thermal decomposition of alkaline-earth and alkali-uranyl oxide hydrates and carbonates commonly produces high-temperature uranates (Čejka and Urbanec 1990; Rogova et al. 1974; Čejka 1969; Brisi and Appendino 1969; Bobo 1964). High-temperature sodium uranates are potentially important nuclear waste forms (Lindemer et al. 1981), and recent interest in the U^{6+} minerals stems from their potential importance as corrosion products of spent UO_2 nuclear fuel (Finch and Ewing 1991). An understanding of the behavior of U^{6+} minerals in nature provides insight into the long-term behavior of structurally and chemically similar nuclear waste forms in a geologic repository (Bruno et al. 1995; Ewing 1993; Finch and Ewing 1991, 1993).

PREVIOUS WORK

Clarkeite was first described by Ross et al. (1931) from the Spruce Pine pegmatite district in western North Carolina, USA, where it replaces uraninite pseudomorphically. Ross et al. derived a general formula for clarkeite, $RO{\cdot}3UO_3{\cdot}3H_2O$, in which R represents alkalis and alkaline earths, predominantly Na. Their formula was based on the basis of wet chemical analyses of two samples from an unspecified pegmatite near Spruce Pine, NC, in which clarkeite is commonly associated with albite, muscovite, and zircon.

Gruner (1954) showed that clarkeite is isostructural with two synthetic high-temperature uranates. One of these is a calcium uranate (of undetermined composition) synthesized by Gruner from aqueous solution at 258 °C. The other uranate was commercially prepared $Na_2U_2O_7$, deficient in Na (8.8 wt% Na_2O instead of the expected 10.36 wt%). Gruner attributed the low Na content to the

* Present address: Argonne National Laboratory, 9700 S. Cass Avenue, Argonne, Illinois 60439, U.S.A.

age of the $Na_2U_2O_7$, prepared 30 years earlier. The synthetic samples gave ''very faint X-ray pattern[s]'', so Gruner heated them to ''low redness'' for up to 5 h, after which the XRD powder patterns for the synthesis products closely resembled that of clarkeite. Gruner suggested that the material of Ross et al. (1931) was impure, and he proposed that the general formula for clarkeite is $(Na,K)_{2-2x}(Ca,Pb)_xU_2O_7{\cdot}yH_2O$.

Gruner considered K and Pb to be impurities in a solid solution between ideal end-member compositions CaU_2O_7 and $Na_2U_2O_7$.

Frondel and Meyrowitz (1956) subsequently described clarkeite from near Rajputana, in the Ajmer district, India. Rajputana clarkeite is richer in Pb, Ca, Th, and U^{4+} than Spruce Pine clarkeite. Frondel and Meyrowitz supported the conclusions of Gruner (1954), but they proposed that H_2O occurs in cation positions and that OH groups replace O atoms, maintaining charge balance. The formula for Rajputana clarkeite (Frondel and Meyrowitz 1956) was reported as

$$(Na_{0.53}Ca_{0.26}Pb_{0.25}Th_{0.06}U^{4+}{}_{0.02}H_2O_{0.88})_{\Sigma 2}U_2(O_{6.87}OH_{0.13})_{\Sigma 7}.$$

Ross et al. (1931) reported approximately 1 wt% rare earth oxides in Spruce Pine clarkeite (including Y_2O_3 and ThO_2), but these were not included in their calculated formula.

Frondel (1958) and Gruner (1954) reported interplanar spacings from XRD powder data for clarkeite, and a two-theta-vs.-intensity XRD stick pattern is given in Ross et al. (1931). All three mineral samples were from near Spruce Pine (unspecified mines), but differences exist among the three powder patterns. Most important, a significant diffraction maximum (40% relative intensity) in the data of Frondel (1958), corresponding to 4.09 Å, is not reported by Ross et al. (1931) or Gruner (1954).

No new data for clarkeite have been reported since 1956, although Frondel (1958) summarized the three earlier studies. The unit-cell parameters and crystal system of clarkeite had not been determined. Clarkeite is rare and occurs intimately intergrown with other U minerals. Because of clarkeite's cryptocrystalline character, detailed characterization is difficult.

Structurally related synthetic sodium uranates

Na predominates over all non-U cations in clarkeite (Ross et al. 1931; Frondel 1958). Four synthetic anhydrous sodium uranates with compositions between Na_2O and UO_3 are known (Lindemer et al. 1981) (Fig. 1). Two of these, $Na_2U_2O_7$ and $Na_6U_7O_{24}$ ($Na_{1.72}U_2O_{6.86}$), are isostructural with clarkeite and are difficult to distinguish using powder XRD (Cordfunke and Loopstra 1971; Toussaint and Avogadro 1974). The structure of synthetic $Na_2U_2O_7$ ($R\bar{3}m$, $a = 3.93$ $c = 17.76$ Å; $Z = 1.5$) (Kovba et al. 1961) is an oxygen-deficient derivative of $CaUO_4$ ($R\bar{3}m$, $a = 3.878$ $c = 17.564$ Å; $Z = 3$) (Loopstra and Rietveld 1969). Both structures are based on sheets of edge-sharing U^{6+} polyhedra consisting of approximately

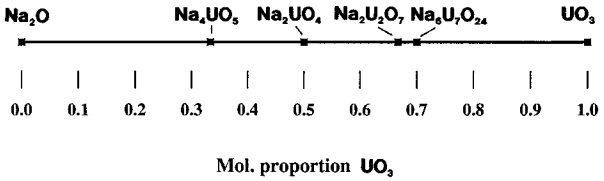

Figure 1. Compositional tie-line between Na_2O and UO_3 showing sodium uranates stable at ~680 °C. Modified after Lindemer et al. (1981).

linear uranyl ions coordinated to six equatorial O atoms parallel to the plane of the structural sheet; Na or Ca atoms occupy interlayer sites. One-fourth of the sheet O atoms are vacant in $Na_2U_2O_7$ in comparison with $CaUO_4$. The unit cell of Kovba et al. (1961) requires that oxygen vacancies in $Na_2U_2O_7$ are disordered, although the many vacancies suggest that the reported unit cell may be a subcell. In fact, Cordfunke and Loopstra (1971) reported a monoclinic unit cell for $Na_2U_2O_7$ synthesized in aqueous solution.

The structure of anhydrous $Na_6U_7O_{24}$ is not known, but, on the basis of XRD powder patterns, it is closely similar to $Na_2U_2O_7$, but with additional O vacancies in the structural sheets and $\frac{1}{7}$ of the Na sites vacant. The hydrated phase, $Na_6U_7O_{24}{\cdot}nH_2O$ ($12 < n < 16$), is formed in aqueous solutions between approximately 25 and 250 °C, and the loss of all H_2O does not significantly change the XRD powder pattern (Wamser et al. 1952). However, Cordfunke and Loopstra (1971) reported a triclinic unit cell for $Na_6U_7O_{24}$ prepared from aqueous solution, whereas Toussaint and Avogadro (1974) reported the $Na_2U_2O_7$–type rhombohedral unit cell for $Na_6U_7O_{24}$ synthesized from an oxide melt at 800 °C. As the XRD powder pattern of anhydrous $Na_6U_7O_{24}$ can be indexed on the same unit cell as $Na_2U_2O_7$ (Toussaint and Avogadro 1974), the formula for $Na_6U_7O_{24}$ is probably more accurately written $Na_{1.72}U_2O_{6.86}$. Notably, the concentration of Na_2O in anhydrous $Na_6U_7O_{24}$ is 8.5 wt%, nearly the same value reported by Gruner (1954) for the synthetic $Na_2U_2O_7$ that he showed to be isostructural with clarkeite.

The structural similarities of $Na_2U_2O_7$, $Na_{1.72}U_2O_{6.86}$, and $CaUO_4$ suggest that Na-Ca substitution is possible; however, few data are available on sodium-calcium uranates. Čejka (1969) reported two rhombohedral high-temperature uranates with XRD powder patterns similar to that of clarkeite, both with equal atomic proportions of Na and Ca. Changing the Ca:Na ratio requires a coupled substitution, such as $2Na^+ \leftrightarrow 2Ca^{2+} + O^{2-}$, but experimental evidence for complete solid solution between Na and Ca end-member uranates is lacking. Limited solid solution of lanthanides in sodium uranates has been reported; e.g., $Na_{0.5}La_{0.5}UO_4$ is isostructural with $CaUO_4$ (Fonteneau et al. 1975).

Sample descriptions

We examined seven museum samples of clarkeite from the Spruce Pine district, Mitchell and Yancey Counties,

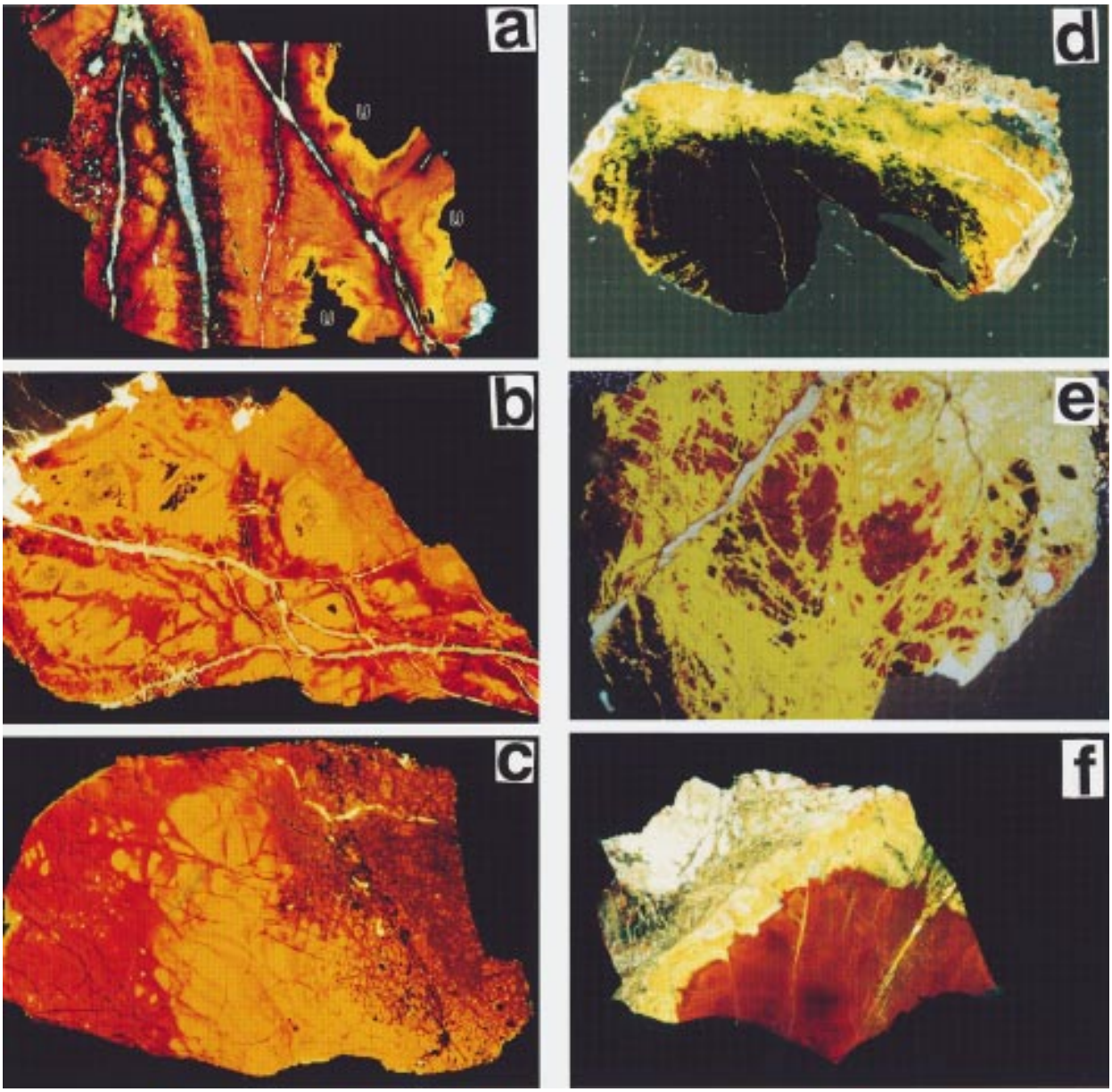

FIGURE 2. Photomicrographs of petrographic thin sections of clarkeite samples. Fields of view for all figures are 1.5 cm across. Transmitted light, crossed polars except (**d**) and (**e**), polars at 45° and oblique reflected light. Sample HM 131885 is not shown. (**a**) DMNH 12228, Fanny Gouge mine, Spruce Pine district, Yancey Co., NC: The three black embayments at right are uraninite (U), each of which is surrounded by a thin region of the K-rich phase (dark yellow) that grades into light brown clarkeite. The dark brown regions are Ca rich and are associated with veins of polycrystalline quartz and minor muscovite; bright inclusions are quartz. (**b**) HM 132290, Spruce Pine district (unspecified mine): Dark brown regions are Ca-rich, lighter regions are clarkeite, veins are primarily quartz; a few remnant uraninite grains (black) are visible within the clarkeite; altered zircon is at upper left. (**c**) HM 132291, Spruce Pine district (unspecified mine): Mixed clarkeite and uraninite (mottled brown) at right grades into yellow-brown clarkeite; dark brown Ca-rich region is at left and contains lighter blebs of clarkeite. A quartz-muscovite vein is visible at upper right. (**d**) CSM 2026.1, Spruce Pine district (unspecified mine): Darkest region at bottom is predominantly clarkeite with admixed Ca-rich material and remnant uraninite. Upper, light yellow region is primarily uranophane with admixed clarkeite. Altered polycrystalline zircon and quartz is at the top, and muscovite is at right. (**e**) DMNH 13283, Spruce Pine district (unspecified mine): Darkest brown to black regions are Ca rich and are surrounded by yellow clarkeite; the lightest regions are uranophane. A quartz vein transects the sample at left. This sample contains inclusions of lead-uranyl oxide hydrates and remnant uraninite grains not apparent at this scale. (**f**) HM 132288, Rajputana, Ajmer district, India (unspecified mine): Dark brown region is Pb- and Ca-rich clarkeite with inclusions of curite. Light yellow band across the center is predominantly uranophane. Uppermost portion of sample is polycrystalline muscovite and quartz; an altered zircon crystal is at top left (white).

TABLE 1. Electron microprobe oxide standards

Oxide analyzed	Standard
UO_3	UO_2 (synthetic)
Na_2O	albite (mineral)
K_2O	K-anorthite (mineral)
CaO, SiO_2, Al_2O_3	andesine (mineral)
PbO	cerussite (mineral)
BaO	benitoite (mineral)
SrO	$SrMoO_4$ (synthetic)
ThO_2	$ThSiO_4$ (synthetic)
ZrO_2	$ZrSiO_4$ (synthetic)
Y_2O_3, Ce_2O_3, La_2O_3	(RE)PO_4 (synthetic)
P_2O_5	apatite (mineral)
MgO	garnet (mineral)

North Carolina, U.S.A. A portion of the sample from Rajputana, India, originally described by Frondel and Meyrowitz (1956) was also analyzed. The clarkeite samples from Spruce Pine are similar in appearance (Fig. 2). Two of these are from the Fanny Gouge mine in Yancey County; the other five are labeled only ''Spruce Pine.'' Other than Fanny Gouge, several currently dormant mines, including the Pink, the Wiseman's, and the Flat Rock, may contain clarkeite (B. Mattison, personnal communication). No mine is indicated for the Rajputana clarkeite. All samples contain micro- to cryptocrystalline clarkeite with coexisting (yellow) uranophane, $Ca[(UO_2)_2(SiO_3OH)_2]\cdot(H_2O)_5$ (Fig. 2).

Clarkeite varies from dark brown to reddish orange in hand specimen. In transmitted light the color varies from brownish yellow to brown, rarely black, and opaque. Opaque clarkeite and uraninite can be distinguished under reflected light or backscattered electron (BSE) imaging; uraninite is more reflective with higher relief and has brighter contrast in BSE images. Opaque regions commonly contain both clarkeite and corroded grains of uraninite. Some samples also contain muscovite, albite, and corroded zircon. All samples are transected by thin veins of quartz (10–500 μm wide) and, less commonly, by thin plates of muscovite (10–100 μm wide) (Fig.2). Samples are labeled with reference to the institution from which they were obtained: ''HM'' refers to the Harvard Mineralogical Museum; ''DMNH'' refers to the Denver Museum of Natural History; ''CSM'' refers to the Geology Museum at the Colorado School of Mines. One sample from the Harvard Museum was not catalogued; it is labeled ''434 (HM)'' here, but this does not correspond to a Harvard catalogue number.

EXPERIMENTAL PROCEDURES

Petrographic thin sections were made for the Rajputana sample and six of the seven Spruce Pine samples. Thin sections were polished using alcohol as a lubricant and were carbon coated under vacuum. Microprobe analyses were performed using an automated JEOL733 Superprobe with five wavelength-dispersion X-ray spectrometers. The microprobe was operated with an accelerating voltage of 15 kV and a beam current of 20 nA. To minimize the volatilization of Na, a beam size of 10 μm was used. This increased sampling from adjacent polycrystalline material and grain boundaries, but smaller beam sizes (1 and 5 μm) gave lower totals and commonly irreproducible results. Beam sizes larger that 10 μm did not improve analytical totals. Raw data were corrected for dead time, drift, fluorescence, and absorption using an empirical α-factor method (Bence and Albee 1968; Albee and Ray 1970). The electron microprobe (EMP) oxide standards are listed in Table 1. Approximate detection limits were 100 ppm for Si, Al, P, Na, and Ca, 150 ppm for Y, Zr, and Th, and 200 ppm for Ce.

FIGURE 3. Backscattered electron image of relict uraninite (bright contrast) partly replaced by clarkeite and K-rich phase (darkest contrast). Bubbles in the uraninite are preserved in the surrounding clarkeite (arrows), suggesting solid-state replacement (sample DMNH 13283). Scale bar at lower right is 100 μm.

Two diffractometers were used to record the XRD powder data. Data for the six samples analyzed by microprobe were collected using a fully automated Scintag powder diffractometer with Bragg-Brentano geometry and a diffracted-beam graphite monochrometer (Cu*K*α radiation) operated at 30 kV and 40 mA. Samples were separated by hand from macroscopic inclusions, ground by hand under acetone, and mounted on a ''zero-background'' oriented quartz holder.

Material from sample 434 (HM) was extracted from a partly altered core of dark red-brown clarkeite using a rotary drill with a stainless steel bit. The powder obtained

TABLE 2. Electron microprobe analyses for clarkeite

	DMNH12228	HM131885	HM132290	HM132290	*HM132290
UO_3	83.14(0.87)	74.61(1.51)	76.97(0.95)	79.63(0.54)	78.88(1.6)
Na_2O	7.01(0.18)	5.09(1.15)	6.19(0.44)	6.11(0.48)	3.58(1.4)
K_2O	0.42(0.03)	0.14(0.02)	0.32(0.07)	0.35(0.11)	0
CaO	0.37(0.16)	0.35(0.08)	0.49(0.47)	0.62(0.71)	5.20(1.10)
PbO	3.96(0.07)	3.56(0.16)	3.94(0.10)	3.83(0.14)	3.94(0.40)
BaO	0	n.d.	n.d.	n.d.	n.d.
SrO	0.29(0.01)	n.d.	n.d.	n.d.	n.d.
ThO_2	0.49(0.03)	0.65(0.22)	0.45(0.03)	0.45(0.05)	0.49(0.08)
ZrO_2	0	n.d.	0	0	0
Y_2O_3	0.82(0.04)	3.05(0.46)	0.97(0.11)	1.15(0.11)	1.06(0.28)
Ce_2O_3	n.d.	0.15(0.02)	n.d.	n.d.	n.d.
SiO_2	0.03(0.04)	0	0	n.d.	0
P_2O_5	n.d.	0	n.d.	n.d.	n.d.
Al_2O_3	n.d.	n.d.	n.d.	n.d.	n.d.
"H_2O"	3.47(diff)	12.40(diff)	10.67(diff)	7.86(diff)	6.85(diff)
Total	96.53	87.60	89.33	92.14	93.15

	DMNH 12228		HM131885		HM132290		HM132290		*HM132290	
	pres.	init.	pres.	init.	pres.	init.	pres.	init.	pres.	init.
"O"	3.344	3.459	3.378	3.494	3.324	3.447	3.330	3.447	3.453	3.573
U	0.942	1.000	0.942	1.000	0.938	1.000	0.942	1.000	0.940	1.000
Na	0.733	0.733	0.593	0.593	0.696	0.696	0.667	0.667	0.394	0.394
K	0.029	0.029	0.011	0.011	0.024	0.024	0.025	0.025	0	0
Ca	0.021	0.021	0.023	0.023	0.030	0.030	0.037	0.037	0.316	0.316
Pb	0.058		0.058		0.062		0.058		0.060	
Ba	0	0	—	—	—	—	—	—	—	—
Sr	0.009	0.009	—	—	—	—	—	—	—	—
Th	0.006	0.006	0.009	0.009	0.006	0.006	0.006	0.006	0.006	0.006
Zr	0	0	—	—	0	0	0	0	0	0
Y	0.024	0.024	0.098	0.098	0.030	0.030	0.034	0.034	0.032	0.032
Ce	—	—	0.003	0.003	—	—	—	—	—	—
"Vac."	0.120	0.356	0.206	0.264	0.152	0.214	0.172	0.230	0.192	0.252
O^{2-}	0.918		0.989		0.894		0.892		1.146	
OH^-	1.082		1.011		1.106		1.108		0.854	
H_2O	0.07		1.67		1.29		0.81		0.78	

Notes: n.d. = not determined, 0 indicates below detection. "O" is the number of O atoms calculated for the anhydrous part of the clarkeite formula. O^{2-} and OH^- are stoichiometric coefficients for the sheet O atoms and OH groups and do not include uranyl O atoms. Columns labeled "pres." refer to the stoichiometric coefficients at the present; those labeled "init." refer to the coefficients at the time of formation. "Vac." is the number of interlayer cation vacancies calculated on the basis of one interlayer cation per formula unit and does not include H_2O. Stoichiometric coefficients are reported to the third decimal place to reduce rounding errors; precision is to two decimal places only.

* Ca-rich material.
** K-rich phase.
† Light-brown material.
‡ Dark-brown material.

was ground by hand under acetone and mounted on a prolene substrate using hair spray as the mounting medium. X-ray data were collected on a Siemens D5000 X-ray diffractometer with a curved Ge crystal incident-beam monochrometer (Cu$K\alpha_1$, λ = 1.5406 Å) operating in transmission (Debye-Scherrer) geometry. Data were collected over the range 6–125°, with a step interval of 0.02° 2θ and a counting time of 20 s per step. Data from sample 434 (HM) were used for Rietveld refinement using the program DBWS (PC version) on the basis of the Rietveld refinement routine of Wiles and Young (1981).

COMPOSITION

Clarkeite from Spruce Pine is zoned compositionally. After U, the most important cations in clarkeite are Na, Ca, and K, and the compositional differences between zones reflect variations in the abundances of these three elements. A small variably sized "core" region, in which K predominates over Na and Ca, is observed in most samples; these are approximately equidistant from surrounding quartz veins. Relict grains of corroded uraninite, when present, occur within this K-rich core, and a 50–100 μm rim of a K-rich phase typically surrounds the uraninite (Fig. 3). Electron microprobe totals for the K-rich phase are lower than for clarkeite (Table 2), and electron beam damage to this phase is more evident than for the surrounding clarkeite. The atomic ratio K/(Na + Ca + K) for the K-rich core (sample DMNH 132291) is 0.784 (Table 2).

Surrounding the K-rich core is clarkeite, for which the atomic ratio Na/(Na + Ca + K) > 0.9 (0.935 for sample DMNH 12228, Table 2); an exception is sample DMNH 13283, for which 0.765 ≤ Na/(Na+ Ca + K) ≤ 0.859 (Table 2). The boundary between clarkeite and the K-rich core is chemically abrupt, although it is not always distinct in transmitted light. The boundary is evident in BSE images (Fig. 3) and is also apparent in reflected light due to the commonly lower relief of the K-rich core. Volu-

TABLE 2—Continued

HM132291	**HM132291	*CSM2026.1	†DMNH13283	‡DMNH13283	HM132288
78.96(0.77)	82.57(1.4)	75.45(0.45)	89.22(0.83)	87.96(0.66)	75.75(0.63)
5.65(0.73)	0.27(1.08)	2.02(0.11)	4.67(0.49)	4.57(0.46)	1.93(0.16)
0.62(0.27)	3.61(0.42)	0.15(0.06)	0.58(0.05)	0.64(0.10)	1.11(0.09)
0.28(0.17)	0.35(0.34)	8.97(0.63)	0.70(0.17)	1.77(0.41)	2.5(0.13)
3.98(0.15)	3.91(0.86)	3.93(0.37)	4.07(0.17)	4.02(0.11)	7.82(0.19)
n.d.	n.d.	0	0	0	0.14(0.15)
n.d.	0.31(0.04)	0.57(0.04)	0.34(0.02)	0.29(0.02)	0.82(0.08)
0.43(0.05)	0.49(0.06)	0.44(0.05)	0.45(0.02)	0.47(0.02)	1.92(0.09)
n.d.	n.d.	0.67(0.11)	0	0	1.02(0.30)
0.98(0.09)	0.84(0.14)	0.76(0.05)	0.72(0.09)	0.68(0.05)	0.28(0.12)
n.d.	n.d.	0	0.06(0.02)	0.05(0.02)	0.02(0.02)
0	0	0	0	0	0
n.d.	n.d.	n.d.	0	0	0.42(0.15)
n.d.	n.d.	n.d.	0	0	n.d.
9.10(diff)	7.65(diff)	7.04(diff)	—	—	6.69(diff)
90.90	92.35	92.96	100.81	100.45	93.31

HM132291		**HM132291		*CSM2026.1		†DMNH13283		‡DMNH13283		HM132288	
pres.	init.	pres.	init.	pres.	init.	pres.	init.	pres.	init.	pres.	init.
3.283	3.405	3.110	3.225	3.361	3.796	3.225	3.335	3.282	3.393	3.205	3.438
0.939	1.000	0.943	1.000	0.937	1.000	0.945	1.000	0.945	1.000	0.883	1.000
0.620	0.620	0.028	0.028	0.232	0.232	0.456	0.456	0.453	0.453	0.208	0.208
0.045	0.045	0.250	0.250	0.011	0.011	0.037	0.037	0.042	0.042	0.079	0.079
0.017	0.017	0.020	0.020	0.568	0.568	0.038	0.038	0.097	0.097	0.149	0.149
0.061		0.057		0.063		0.055		0.055		0.117	
—	—	—	—	0	0	0	0	0	0	0.003	0.003
—	—	0.016	0.016	0.020	0.020	0.010	0.010	0.009	0.009	0.026	0.026
0.006	0.006	0.006	0.006	0.006	0.006	0.005	0.005	0.005	0.005	0.024	0.024
—	—	0	0	0.020	0.020	0	0	0	0	0.028	0.028
0.030	0.030	0.024	0.024	0.024	0.024	0.019	0.019	0.019	0.019	0.008	0.008
—	—	—	—	0	0	0.001	0.001	0.001	0.001	0.000	0.000
0.222	0.283	0.597	0.654	0.057	0.120	0.378	0.433	0.320	0.375	0.358	0.475
0.813		0.446		1.595		1.335		1.393		0.875	
1.187		1.554		0.405		—		—		1.125	
0.97		0.51		1.09		0		0		0.59	

metrically, clarkeite is the most important constituent in the Spruce Pine samples and comprises approximately 70–90 vol% of the clarkeite samples.

Clarkeite is commonly rimmed and veined by Ca-rich material that is dark brown to nearly black with low birefringence. Ca-rich regions appear polycrystalline in transmitted light and may be impure. The atomic ratio Ca/(Na + Ca + K) varies among samples, from 0.445 (sample DMNH 132290) to 0.700 (sample CSM 2026.1) (Table 2), but is more or less constant within a single sample. Na exceeds Ca in most samples, although Ca predominates in CSM 2026.1 (Table 2). K is a minor component in all analyses of the Ca-rich material. The Ca-rich regions are always closely associated with quartz veins, with widths ranging from approximately 50 μm to approximately 1 mm (Fig. 2). The boundary between the Ca-rich material and clarkeite is gradational, both optically and compositionally.

TABLE 3. Electron microprobe analysis (wt%) for Spruce Pine uraninite

UO_2	88.52(1.37)
PbO	4.50(0.05)
CaO	0.20(0.01)
Na_2O	0.11(0.11)
K_2O	0.14(0.03)
Y_2O_3	1.06(0.13)
ThO_2	0.50(0.02)
Total	95.03

Note: Sample HM 132290. SiO_2, La_2O_3, and ZrO_2 below detection; BaO, SrO not determined; U reported as UO_2.

Pb and Th exhibit no significant variation between compositional zones. The atomic ratios Pb:U and Th:U are approximately equal in all Spruce Pine samples and constant across the zones (Table 2); they are also equivalent to Pb:U and Th:U atomic ratios in the primary uraninite, when present (Table 3). Y is considerably more variable between samples (Table 2); however, it is more or less constant across zones within each sample. Ce was determined for only four samples, but variations among samples are not significant within the detection limit (Table 2).

Figure 4 shows the results of an EMP traverse from a quartz-filled vein to the edge of an altered uraninite grain in sample DNMH 12228; atomic proportions are normalized to U. This illustrates the variation of Na, Ca, K, and Pb commonly observed across compositional zones. Ca is highest nearest the quartz vein, decreasing as Na increases toward the remnant uraninite. Na decreases abruptly where K increases in the region immediately adjacent to remnant uraninite. Pb remains constant across all three compositional zones.

Analytical totals are variable, both within and between

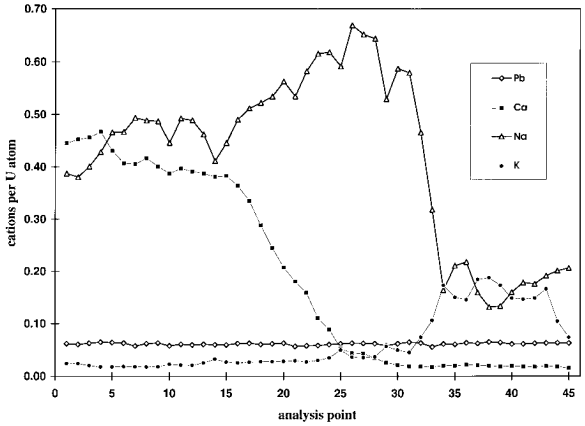

FIGURE 4. Plot of EMPA traverse showing molar proportions of the major constituents in clarkeite. Traverse is from near a quartz vein (**left**) to the edge of an altered uraninite grain (**right**). Distance between analysis points is approximately 40 μm (sample DMNH 12228).

samples. Low totals may be due to the cryptocrystalline nature of clarkeite. Absorbed H_2O at grain boundaries can reduce analytical totals, and may be especially problematic for fine-grained materials. In addition, the surfaces of the polished sections were not ideally flat due to difficulties when polishing polycrystalline materials. Though surface roughness was not severe for the clarkeite samples, it may have contributed to the poor analytical totals. Uneven surfaces of probe sections, caused by differences in hardness among compositional zones and mineral inclusions, also affected analytical results. The H_2O content was estimated by difference and is highly variable (and may be overestimated in some analyses). Analyses of optically homogeneous material usually indicate H_2O contentsof 0–2 moles H_2O per mole U. On average, H_2O contents reported here are higher than those reported by Ross et al. (1931), Frondel and Meyrowitz (1956), and Frondel (1958) (Table 2). Analytical totals for sample DMNH 13283 were near 100% for both the yellow-brown core material and the darker brown material (Table 2). This sample was also enriched in U and depleted in Na in comparison with the other clarkeite samples. The XRD powder pattern for this sample is indistinguishable from the other Spruce Pine clarkeite samples; however, it was not possible to obtain sufficiently pure material for detailed XRD analysis. Sample DMNH 13283 is marked only ''Spruce Pine'' with no indication of the mine from which it was collected.

XRD DATA

Discrepancies among published XRD patterns for clarkeite required us to infer the actual clarkeite XRD powder pattern by identifying diffraction maxima common among the samples in this study, and by comparing the powder patterns with the reported patterns. Clarkeite is intimately intergrown with other minerals, and single phase specimens could not be obtained for XRD analysis.

TABLE 4. Unit-cell parameters (Å) of clarkeite and related synthetic uranates

	Clarkeite*		Synthetic high-temperature uranates		
	Spruce Pine	Rajputana	$Na_{1.72}U_2O_{6.86}$ [1]	$CaUO_4$ [2]	**α-U_3O_8 [3]
Rhombohedral unit cell					
a	6.335(3)	6.37(2)	6.36	6.268	—
α	35.38(1)°	36.44(2)°	36.17°	36.04°	—
Hexagonal unit cell†					
a	3.954(4)	3.98(1)	3.95	3.878	3.905
c	17.73(1)	17.81(5)	17.82	17.564	4.146 (γ = 118.6°)
Orthorhombic pseudo-cell‡					
a	6.848(7)	6.89(2)	6.84	6.717	6.716
b	11.862(3)	11.94(3)	11.82	11.611	11.960
c	17.73(1)	17.81(5)	17.82	17.564	4.146

Notes: [1] Toussaint and Avogadro (1974); [2] Loopstra and Rietveld (1969); [3] Loopstra (1970a). γ for pseudohexagonal unit cell of α-U_3O_8.

* Spruce Pine: DMNH 12228; Rajputana: HM 132288.

** α-U_3O_8 is truly orthorhomibic and cannot be indexed on a clarkeite-type rhombohedral cell.

† Unit-cell parameters of clarkeite were refined on the hexagonal cell.

‡ The hexagonal-to-orthorhombic transformation is $a_O = a_H\sqrt{3}$; $b_O = 3a_H$; $c_O = c_H$. This allows comparison with α-U_3O_8.

However, separation of samples by hand according to color (dark orange to reddish brown) provided material that consistently produced similar XRD powder patterns.

Diffraction maxima are broad, and broad basal ''humps'' are commonly associated with three clusters of interplanar spacings (4.0–2.6, 2.1–1.8, and 1.8–1.5 Å). Only these three broad humps are evident in the powder pattern for dark orange clarkeite from sample HM 132291. Quartz is a common inclusion and was readily identified in the powder patterns. The most common uranium minerals other than clarkeite evident in the XRD powder patterns are uranophane and wölsendorfite, although uraninite, curite, becquerelite, and an undetermined lead-uranyl oxide hydrate (fourmarierite or vandendriesscheite) are also common (these minerals were also identified by EMPA). Curite and wölsendorfite do not occur together; rather, wölsendorfite is common within the Spruce Pine clarkeite samples, whereas curite is abundant in the Rajputana sample.

The 4.09 Å *d* value reported for Spruce Pine clarkeite by Frondel (1958) was not observed in XRD patterns of any of our samples, nor was it reported by Ross et al. (1931) or Gruner (1954). This *d* value is also absent from data for the synthetic high-temperature uranates structurally related to clarkeite (Table 4). We consider this *d* value spurious and not characteristic of clarkeite. Unfortunately, the only pattern for clarkeite in the current ICDD data base includes the 4.09 Å *d* value (PDF 8-315).

Clarkeite from the Fanny Gouge mine near Spruce Pine (DMNH 12228) provided material of sufficient purity to permit unit-cell parameters to be determined and refined. The powder pattern was readily indexed on the hexagonal unit cell reported for $Na_{1.72}U_2O_{6.86}$ (space group $R\bar{3}m$, 166) (Toussaint and Avogadro 1974). We were not able to in-

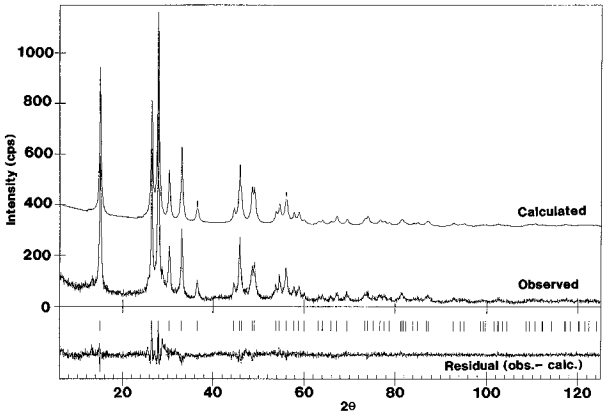

FIGURE 5. Calculated (**top**), observed (**middle**) and residual (**bottom**) plots of XRD data for clarkeite sample 434 (HM). Vertical marks indicate positions of allowed Bragg reflections.

dex the clarkeite powder pattern using the monoclinic or triclinic unit-cell parameters reported by Cordfunke and Loopstra (1971) for $Na_2U_2O_7$ and $Na_6U_7O_{24}$, respectively. Refined unit-cell parameters for the Spruce Pine clarkeite are given in Table 4. Unit-cell parameters were also refined for the Rajputana clarkeite (HM 132288), but this sample is impure and contains substantial curite and uranophane. The unit-cell parameters reported for sample HM 132288 are therefore considered approximate, but they are nonetheless comparable to those of clarkeite from the Fanny Gouge mine (Table 4).

The powder XRD data and chemical analyses indicate that clarkeite is isostructural with $Na_{1.72}U_2O_{6.86}$ (Toussaint and Avogadro 1974), $CaUO_4$ (Loopstra and Rietveld 1969) and $Na_{0.5}La_{0.5}UO_4$ (Fonteneau et al. 1975) (Table 4). Unfortunately, sufficiently pure clarkeite from DMNH 12228 could not be obtained for a suitable structure refinement using the method of Rietveld (1969) and this was performed using sample 434 (HM). The composition of sample 434 (HM) was not determined.

RIETVELD REFINEMENT

Structural parameters from $CaUO_4$ (Loopstra and Rietveld 1969) and $Na_{0.5}La_{0.5}UO_4$ (Fonteneau et al. 1975) were used as starting models for the structure of clarkeite, and both yielded identical refinement results. Cation-site occupancies were released independently, one at each step (while holding the scale factor fixed) and then refined simultaneously (with the scale factor released). The U-site occupancy was refined together with that of the uranyl O atom, O1 (that is, as the uranyl ion, UO_2^{2+}). The uranyl-ion occupancy decreased slightly, but not to the value of ~0.94 U apfu expected on the basis of EMP analyses (Table 2). The Na-site occupancy increased slightly, consistent with Ca, REE, and Pb substitution at the Na site.

The site occupancy of the sheet O atom, O2, decreased to 88% of the starting value, from 2 to 1.76 apfu, a value significantly higher than that calculated for sample DNMH 12228 based on only O^{2-} ions in the structural unit: 1.46 O apfu. This lower O2-site occupancy is not sufficient evidence for reduced uranyl ion coordination in clarkeite in comparison with $CaUO_4$, as the XRD powder data are not of sufficient quality to refine O-site occupancies confidently in the presence of U. Occupancies are correlated with displacement factors, but our data do not permit the refinement of displacement factors, and we used B_{iso} values for $CaUO_4$ (Loopstra and Rietveld 1969).

The observed and calculated XRD powder patterns and difference plot for the final refinement are illustrated in Figure 5. The final refinement *R* values and unit-cell parameters are reported in Table 5, and selected bond lengths are in Table 6. The indexed powder pattern, relative intensities, and structure factors are listed in Table 7.

Notably, the ratio of sheet O atoms (including OH groups) to uranyl ions in the uranyl-oxide hydrates fourmarierite and schoepite is 1.75, and both minerals have fivefold-coordinated uranyl ions (Piret 1985; Finch et al. 1996a). Fourfold- and fivefold-coordinated uranyl ions are common among low-temperature uranyl-oxide hydrates (Burns et al. 1996), since this decreases steric crowding in the structural sheets of uranyl compounds in comparison with sixfold-coordinated uranyl ions (Evans 1963). An ordered arrangement of such coordination polyhedra is not compatible with the unit cell and space group $R\bar{3}m$, but an orthorhombic or hexagonal supercell, with uranyl ions in the same relative positions as for the $R\bar{3}m$ cell, might accommodate such an arrangement (Loopstra 1970a and 1970b). Our efforts to refine the structure of clarkeite on such supercells were unsuccessful; however, a disordered arrangement of fivefold-coordinated uranyl ions would resemble the structure proposed for α-$UO_3 \cdot 0.75H_2O$ (''dehydrated schoepite'') in

TABLE 5. Refinement *R* factors and unit-cell parameters for Spruce Pine clarkeite, 434 (HM)

R_{Bragg}	9.50	*a*	3.954(1) Å
R_P	13.99	*c*	17.660(3) Å
R_{WP}	18.27	*V*	239.14 Å^3
R_{WP} (expected)	13.71	*Z*	3[Na(UO_2)O(OH)]
GoF (R_{WP}-R_{WP} (exp'd))	1.33	$\rho_{calc.}$	6.74* g·cm^{-3}
		$\rho_{meas.}$	6.39†–6.29‡ g·cm^{-3}

* Density calculated for the empirical formula for sample DMNH 12228 (Table 2):
$\{Na_{0.733}K_{0.029}Ca_{0.021}Sr_{0.009}Y_{0.024}Th_{0.006}Pb_{0.058}\}[(UO_2)_{0.942}O_{0.918}(OH)_{1.082}](H_2O)_{0.069}$.
† Spruce Pine clarkeite, Ross et al. (1931).
‡ Rajputana clarkeite, Frondel and Meyrowitz (1956).

TABLE 6. Atomic positions and selected bond lengths for Spruce Pine clarkeite, 434 (HM)

Atom	(*x*,*y*,*z*)	B_{iso}*	Bond lengths (Å)	
U	0,0,0	0.29	U-O1	1.90(2) × 2
Na	0,0,½	0.54	U-O2	2.29(2) × 6
O1 (uranyl)	0,0,0.1069	0.42	Na-O1	2.51(1) × 6
O2 (sheet)	0,0,0.3488	0.42	Na-O2	2.75(2) × 2

* Displacement factors from Loopstra & Rietveld (1969) for $CaUO_4$, not refined.

TABLE 7. Observed and calculated intensities and structure factors for clarkeite

hkl	d(Å)$_{obs}$	I/I_{obs}	I/I_{calc}	F_{obs}	F_{calc}
003	5.903	64	63	1915.1	1865.9
101	3.365	56	55	1874.2	1782.7
012	3.195	100	100	2653.2	2567.0
006	2.945	28	25	2654.8	2411.0
104	2.707	34	39	1870.9	1950.0
015	2.460	8	11	990.6	1199.7
107	2.031	8	8	1225.5	1171.2
110	1.9772	33	35	2612.4	2621.7
009	1.9624	4	5	1609.7	1614.5
113	1.8742	19	19	1527.7	1501.2
018	1.8554	19	19	2106.7	2029.5
021	1.7040	8	7	1517.6	1350.8
202	1.6807	14	13	2038.3	1898.8
116	1.6410	23	23	1930.8	1891.5
024	1.5961	8	7	1650.3	1565.1
1010	1.5694	9	9	1747.9	1639.1
205	1.5405	3	3	1110.8	1027.8
0012	1.4715	2	2	1657.7	1580.8
0111	1.4534	3	3	1168.8	1130.4
027	1.4164	2	2	936.7	989.7
119	1.3925	6	8	1203.0	1278.9
208	1.3527	6	6	1711.4	1591.9
211	1.2905	4	4	1094.6	1065.2
122	1.2803	8	8	1466.0	1469.6
1013	1.2625	1	1	796.9	736.6
214	1.2417	6	5	1324.8	1254.6
0210	1.2290	3	3	1420.8	1323.5
125	1.2150	2	2	876.9	851.2
0114	1.1834	3	2	1283.3	1168.1
1112	1.1803	6	5	1403.0	1283.5
0015	1.1771	<1	<1	887.9	818.5
2011	1.1709	2	1	996.0	926.4
217	1.1513	2	2	895.6	818.0
030	1.1412	2	2	1600.9	1477.6
033	1.1203	1	1	1044.6	932.0
128	1.1163	6	5	1437.6	1268.7
036	1.0640	1	1	1345.6	1179.9
0213	1.0640	2	2	720.0	631.3
1016	1.0504	2	1	1074.8	944.4
2110	1.0437	4	3	1212.4	1075.9
2014	1.0154	2	1	1101.0	966.4
1115	1.0114	2	1	774.2	685.0
1211	1.0075	2	2	834.0	759.3
0117	0.9940	1	1	799.9	728.4
220	0.9884	2	2	1298.2	1175.3
039	0.9865	1	1	914.2	824.4
0018	0.9810	1	<1	1079.9	979.1
223	0.9747	2	2	817.3	754.0
131	0.9482	1	1	739.8	695.9
312	0.9442	3	3	1018.1	948.5
226	0.9370	1	1	1033.1	957.3
2113	0.9370	3	3	573.7	531.6
134	0.9284	2	2	924.8	833.8
0216	0.9276	1	1	876.8	788.5
315	0.9171	1	1	681.1	576.7
1214	0.9033	3	2	939.8	793.2
0312	0.9019	2	1	1006.1	852.2
1019	0.8970	1	1	630.9	537.3
137	0.8888	1	1	639.2	541.6
2017	0.8881	1	1	692.0	588.5
229	0.8828	2	1	737.0	644.3
1118	0.8788	3	2	876.2	763.0
318	0.8724	2	2	831.3	719.6

Note: Space group $R\bar{3}m$, indexed on hexagonal axes. Sample 434 (HM).

which ⅛ of the sheet O atoms are vacant (Finch et al. 1996b) and for which the ratio of sheet O atoms plus OH groups to uranyl ions is also 1.75.

The *z* coordinates of both O atoms were refined (cations are on special positions). The final U-O1 distance is 1.90 Å, shorter than the U-O1 bond in $CaUO_4$ (1.963 Å, Loopstra and Rietveld 1969) but longer than reported for most low-temperature uranyl-oxide hydrates: 1.75−1.85 Å (Taylor 1971; Mereiter 1979; Piret-Muenier and Piret 1982; Piret et al. 1983; Piret 1985; Pagoaga et al. 1987; Finch et al. 1996a). The U-O2 bond distance is 2.29 Å, and the O2 *z* coordinate is consistent with a less puckered arrangement of O2 atoms around the uranyl ions in clarkeite than in $CaUO_4$ (Table 6). Assuming sixfold-coordinated uranyl ions, the O-O distance within the structural sheet is 2.31 Å, which is probably unreasonably close (the closest O-O distance reported for sixfold-coordinated uranyl ions is 2.45 Å in α-$UO_2(OH)_2$; Taylor 1971). However, space-group symmetry dictates that the O2 atom position must adjust perpendicular to the structural sheet only, and possible lengthening of U-O2 distances because of positional disorder or a supercell could not be evaluated.

Difference-Fourier sections through the O2 positions showed minor smearing of the electron density, but this may reflect inappropriate displacement factors because of poor data quality rather than positional disorder.

Bond-valence contributions were calculated assuming each uranyl ion is bonded to six equatorial O atoms (bond-valence parameters from Brown 1981). Bond-valence sums indicate that U is overbonded (6.55 v.u.), though this is common for uranyl compounds (Taylor 1971; Pagoaga et al. 1987; Finch et al. 1996a); O1 is slightly underbonded (1.83 v.u.). The bond-valence contributions to Na and O2 are nearly ideal (1.04 and 1.97 vu, respectively), suggesting that the bonding environments around Na and O2 in clarkeite are similar to comparable sites in $CaUO_4$. Refined O2 occupancies suggest that the coordination for each U atom is on average less than six; however, bond-valence curves for Ure not of sufficient accuracy to permit confident estimation of U atom coordination from bond-valence sums.

An important drawback to the Rietveld refinement of clarkeite is the inability to detect deviations from the ideal structure model using powder XRD. Clarkeite is isostructural with a simple, high-symmetry phase, $CaUO_4$, with U atoms on special positions, and X-ray scattering from the U atoms dominates the diffraction pattern, accounting for most of the Bragg intensities. Extraneous diffraction peaks, attributed to minor impurities (Fig. 5), also contribute to uncertainties in the refinement, as additional diffraction peaks may be caused by supercell reflections. Another problem with the refinement was the correct modeling of peak shapes, as indicated by the high value of the whole-pattern agreement index, R_{wp} (Table 5). (The refinement employed a pseudo-Voigt profile-shape function, for which the Gaussian and Lorentzian components were refined together.) Difficulties with modeling peak shapes was exacerbated by broad diffraction maxima and a high degree of peak overlap.

DISCUSSION

Clarkeite is depleted in Na relative to $Na_2U_2O_7$ and $Na_{1.72}U_2O_{6.86}$ ($Na_6U_7O_{24}$) but is enriched in several other

elements (Ca, Sr, Th, Y, Pb, REE). The atomic ratio Pb: U is 0.06 in all of the Spruce Pine samples regardless of zone and is identical to the primary uraninite, when present (Table 3). The Pb in clarkeite was not derived from the primary uraninite during formation, supporting the conclusion of Ross et al. (1931) that clarkeite formed during late-stage pegmatite crystallization, before uraninite accumulated significant radiogenic Pb. Although the leaching of radiogenic Pb from the uraninite by hydrothermal fluids during clarkeite formation cannot be excluded from consideration, the interiors of relict uraninite grains show little or no evidence for chemical alteration; Na, K, and Ca concentrations are the same as for unaltered uraninite from Spruce Pine (Table 3). Furthermore, the ''chemical age'' of the Spruce Pine clarkeite, calculated on the assumption that all Pb is radiogenic (derived from Th and U), indicates a formation of approximately 360–380 Ma, the same as for the uraninite and consistent with the geologic age of the associated igneous rocks.

The atomic ratios Th:U and Y:U are also nearly constant, regardless of zone. These elements were derived from the primary uraninite, suggesting that they were not mobile during the hydrothermal alteration of uraninite. Instead, the replacement of uraninite by clarkeite occurred in situ by metasomatic replacement. This is also supported by the preservation of textures (e.g., relict grain boundaries and bubbles, Fig. 3) that are continuous in both the relict uraninite and the surrounding clarkeite.

As clarkeite formed without Pb, the original composition of clarkeite is calculated by assuming the relationship $U_p + Pb = U_i$, in which U_p is the number of atoms of U at the present time and U_i is the number of U atoms at the time of formation (only a minor error is introduced by ignoring the contribution from Th). Thus, at the time of formation the formula for clarkeite from the Fanny Gouge mine (sample DMNH 12228), calculated on the basis of one U apfu, was:

$$(Na_{0.733}K_{0.029}Ca_{0.021}Sr_{0.009}Y_{0.024}Th_{0.006})UO_{3.459}\cdot 0.61H_2O.$$

The number of O atoms in the anhydrous portion of the clarkeite formula is between that in $Na_{1.72}U_2O_{6.86}$ ($Na_{0.86}UO_{3.43}$) and $Na_2U_2O_7$ ($NaUO_{3.5}$). Only 0.822 interlayer cation sites were filled at the time of formation, compared with 0.86 in $Na_{1.72}U_2O_{6.86}$. Some cation vacancies compensate for the presence of cations with valences greater than +1. The net additional charge due to Ca^{2+}, Sr^{2+} (+1), Y^{3+} (+2), and Th^{4+} (+3) is +0.096, leaving 0.082 more vacancies than required by charge balance on the O atoms only.

The hydrothermal formation of clarkeite suggests that some (or most) H_2O is present as OH. The structural sheets in clarkeite may accommodate OH, with excess H_2O occupying interlayer positions. The structural unit of clarkeite is of the form $[(UO_2)(O,OH)_2]$, that is, with sixfold-coordinated uranyl ions (conclusive evidence for reduced uranyl-ion coordination is lacking). The structural sheets in clarkeite resemble those in $CaUO_4$ and α-$UO_2(OH)_2$, and variable interlayer cation charges are accommodated by adjusting the relative number of O^{2-} ions and OH groups in the structural unit in clarkeite. The general formula for clarkeite when formed is therefore

$$\{(Na,K)_pM^{2+}_qM^{3+}_rM^{4+}_s\}[(UO_2)O_{1-y}(OH)_{1+y}](H_2O)_z,$$

where Na >> K and $p > (q + r + s)$. There is no obvious constraint on z, and the structural role of H_2O in uranyl minerals suggests that H_2O groups do not necessarily occupy cation-equivalent positions (Piret 1985; Pagoaga et al. 1987; Finch et al. 1996a). The value of y is determined by the total charge of the interlayer cations, with $y = 0$ corresponding to a net interlayer charge of +1. For sample DMNH 12228, charge balance requires $[-2(1 - y) - (1 + y)] = -2.918$, or $y = 0.082$. In general: $y = 1 - (p + 2q + 3r + 4s)$. Thus the structural formula for Spruce Pine clarkeite (sample DMNH 12228) at the time of formation was:

$$\{Na_{0.733}K_{0.029}Ca_{0.021}\ Sr_{0.009}Y_{0.024}Th_{0.006}\}_{\Sigma 0.880}$$
$$[(UO_2)O_{0.918}(OH)_{1.082}](H_2O)_{0.069}.$$

Compositional zones

The observed compositional zoning suggests a miscibility gap between clarkeite and a phase that is more Ca rich. The Ca-rich regions are not chemically homogeneous, and the ratio Ca/(Na + Ca) of the Ca-rich regions varies widely between samples (Table 2). These Ca-rich regions may contain a fine-scale mixture of clarkeite and a Ca analogue of clarkeite with ideal composition close to $CaUO_4$ or possibly $Ca_{0.5}Na_{0.5}UO_{3.75}$. The latter formula is that of a synthetic high-temperature uranate structurally related to clarkeite (Čejka 1969).

More work is required to establish the composition of the Ca-rich material. Although structurally similar, clarkeite and the Ca-rich phase must differ with respect to the proportion of O^{2-} ions and OH groups in the structural unit (Table 2). Close similarities in XRD powder patterns of $Na_{1.72}U_2O_{6.86}$ and $CaUO_4$, combined with broad diffraction maxima and the small volume proportion of the Ca phase, prevented the resolution of diffraction maxima belonging to clarkeite and the Ca analogue.

The limited solubility of K in clarkeite may be due to the difference in size between Na^+ and K^+. The solubility limit of K in anhydrous $Na_{1.72}U_2O_{6.86}$ is only 5 mol% above 800 °C (Toussaint and Avogadro 1974), a value similar to that of clarkeite (3 mol% K). Structural differences between the K-rich phase and clarkeite are evident from the higher birefringence and lighter color of the K-rich core, as well as from their different compositions (Table 2). The composition of the K-rich phase resembles that of compreignacite, $K_2[(UO_2)_6O_4(OH)_6](H_2O)_8$, though the K-rich phase appears less hydrated than compreignacite. The formation of the K-rich core is problematic. The close association with relict uraninite grains indicates a genetic relationship, but the nature of this relationship is uncertain, especially because the uraninite contains almost no K (Table 3). Unfortunately, the small volume fraction of the K-rich phase prevented detailed analysis.

The formation of clarkeite

The metasomatic alteration of uraninite by hydrothermal alkali solutions resulted in the pseudomorphic replacement of uraninite by clarkeite. The volume of the reduced rhombohedral cell for Spruce Pine uraninite ($Z = 1$) is 0.402 Å^3, which is one-half that of the rhombohedral unit cell of clarkeite ($Z = 1$): 0.80 Å^3. Thus, Na replaced U, and the conversion of uraninite to clarkeite resulted in the loss of one-half of the U from uraninite.

The formation of clarkeite requires the oxidation of the U^{4+} in uraninite to U^{6+} in clarkeite. However, significant free oxygen is unlikely in deep-seated hydrothermal fluids. The oxidation of U^{4+} by H_2O is thermodynamically unfavorable at 25 °C ($U^{4+} + 2H_2O \rightarrow UO_2^{2+} + 2H^+ + H_2$; $\Delta E = -1.0952$ V) but may be favorable under hydrothermal conditions, allowing H_2O to act as an oxidant. In addition, the solubility of uraninite increases substantially in acid solutions (pH < 4), and the reduction of H^+ by U^{4+} becomes possible, with H_2 diffusing from the system. The reaction by which clarkeite replaces uraninite is: $2UO_{2(cr)} + Na^+ + H^+ + 2H_2O \rightarrow Na[(UO_2)O(OH)]_{(cr)} + (UO_2)^{2+} + 2H_{2(g)}$ (idealized stoichiometries are used for uraninite and clarkeite). The result is an increase in pH. The solutions responsible for the formation of clarkeite were probably low pH, saline brines.

Alpha radiolysis of water may contribute to the oxidation of U^{4+}; however, radiolysis alone would be insufficient to oxidize the uraninite completely, as this is not observed for more ancient uraninites in reducing environments (Janecek and Ewing 1992). Whatever the oxidant, one effect of the replacement reaction was the removal of one-half of the U originally present in uraninite. The fate of the dissolved U is uncertain, but uranyl silicates and uranyl phosphates fill fractures in several Spruce Pine pegmatites and in the surrounding country rocks (Frondel 1956).

The temperature and pressure under which clarkeite formed are uncertain. The late-stage pegmatite fluids probably contained abundant dissolved Si in addition to Na and Ca. The stability of uranyl silicates under hydrothermal conditions is not well known but uranophane and related uranyl silicates are readily synthesized in the temperature range 160–180 °C (Gruner 1954; Cejka and Urbanec 1990; Vochten et al. 1996). The upper temperature limit for uranyl-silicate stability must be below the temperature at which clarkeite formed (uranophane is a weathering product and is not associated with the metasomatism that formed the clarkeite; Frondel, 1956). The equilibrium, sodium boltwoodite ↔ clarkeite + quartz, must be shifted to the right under the temperature and pressure conditions prevailing during clarkeite formation, a conclusion supported by the close association of clarkeite with quartz-filled veins. We therefore suggest that clarkeite formed above ~200 °C.

The role of radiogenic lead

As U decays to Pb, the Pb enters cation vacancies in the interlayer, leaving a U vacancy in the structural sheet. This reflects the dramatically different crystal-chemical characteristics of Pb^{2+} and U^{6+}. Although overall charge balance is probably maintained by the reaction, $(UO_2)^{2+} \rightarrow Pb^{2+} + O_2$, with oxygen diffusing from clarkeite, sheet O atoms surrounding the uranyl vacancy become strongly under-bonded, and the sheet structure is locally destabilized.

The current composition of Spruce Pine clarkeite (sample DMNH 12228) (Table 2) is $\{Na_{0.733}K_{0.029}Ca_{0.021}Sr_{0.009}Y_{0.024}Th_{0.006}Pb_{0.058}\}[(UO_2)_{0.942}O_{0.918}(OH)_{1.082}](H_2O)_{0.069}$. The Pb is radiogenic, and the general formula for clarkeite is $\{(Na,K)_pM^{2+}_qM^{3+}_rM^{4+}_sPb_x\}[(UO_2)_{1-x}O_{1-y}(OH)_{1+y}](H_2O)_z$. As x increases, clarkeite recrystallizes to low-temperature, uranyl-oxide hydrates. Wölsendorfite, $(Ca,Pb)U_2O_7 \cdot 2H_2O$, or curite, $[Pb_{6.56}(H_2O,OH)_4]\,[(UO_2)_8O_6(OH)_8]_2$, are evident in several clarkeite XRD powder patterns, and Pb-rich lamellae, probably curite, are evident in BSE images of the Rajputana clarkeite. Frondel (1956) also reported lead-uranyl oxide hydrates (later shown to include wölsendorfite; Deliens 1977) with Spruce Pine clarkeite.

The limit for x in the formula for clarkeite is not known but probably cannot exceed the number of interlayer cation vacancies initially present; however, the loss of U from the structural sheets probably affects the structure of clarkeite more significantly than adding Pb to the interlayer. The value of x for sample DMNH 12228 (0.058) is slightly less than one-half the number of cation vacancies (0.120) (Table 2), whereas the value of x for the Rajputana sample (0.117) is significantly less than the number of cation vacancies (0.358) (Table 2). On the other hand, the stoichiometric coefficient on the uranyl ion (UO_2) is lower for the Rajputana clarkeite (0.883), and the decomposition of this sample (HM 132288) appears more advanced than for the Spruce Pine clarkeite, for which $x = 0.942$ (Table 2). Curite comprises approximately 20–30 vol% of the Rajputana sample, whereas Spruce Pine clarkeite contains only 5–10 vol% wölsendorfite.

Finally, sample DMNH 13283 requires a separate note. The analytical totals (~100 %) and composition of this sample distinguish it from other Spruce Pine clarkeite samples; DMNH 13283 is significantly more enriched in UO_3. Two analyses are reported in Table 2 for sample DMNH 13283: one from the light brown regions and the other from the darker regions. Both are Na rich and therefore (predominantly) clarkeite (Table 2). The stoichiometries for these analyses do not correspond to the stoichiometries proposed above but are nearly equivalent to $M^+_2(UO_2)_3O_4$ (assuming $U_p = U_i + Pb$). The powder XRD pattern is indistinguishable from powder XRD patterns of clarkeite from other samples. We have no explanation for the compositional difference. The mine from which the sample was collected is unknown, nor does sample DMNH 13283 resemble the samples from the Fanny Gouge mine (Fig. 2).

Low-temperature alteration of clarkeite

Clarkeite occurs intimately intergrown with numerous U^{6+} minerals. The recrystallization of clarkeite because

the accumulation of radiogenic Pb produces curite and wölsendorfite, both of which are also common weathering products of Pb-bearing uraninite. Curite and wölsendorfite have high Pb:U ratios and relatively low molar proportions of H_2O, consistent with formation directly from clarkeite. Other uranyl minerals identified with clarkeite include vandendriesscheite ($PbO{\cdot}7UO_3{\cdot}12H_2O$) or fourmarierite ($Pb[(UO_2)_4O_3(OH)_4](H_2O)_4$), becquerelite ($Ca[(UO_2)_6O_4(OH)_6](H_2O)_8$), and, most abundant, uranophane ($Ca[(UO_2)_2(SiO_3OH)_2](H_2O)_5$). The high H_2O content of many of these minerals indicates that they formed during recent weathering (also see Frondel 1956).

Uranophane commonly occurs within the quartz veins and replaced clarkeite along broad reaction fronts. A narrow (10–200 μm) band of fine-grained (<1–5 μm) uranyl minerals commonly occurs at the reaction front between uranophane and clarkeite. The minerals comprising this reaction front were not positively identified, but qualitative energy-dispersive X-ray (EDS) analyses indicated a mixture of a lead-uranyl oxide hydrate, such as curite, wölsendorfite, or fourmarierite, plus becquerelite (based on Pb:U and Ca:U peak ratios in EDS). Si was also detected along the reaction front, although this may be due to adjacent uranophane. Minor kasolite, $Pb[(UO_2)(SiO_4)](H_2O)$, occurs as inclusions within uranophane, rarely within quartz veins, and (possibly) along the reaction fronts between clarkeite and uranophane.

Although sodium boltwoodite, $Na[(UO_2)(SiO_3OH)](H_2O)$, is structurally related to uranophane (Stohl and Smith 1981; Vochten et al. 1996), sodium boltwoodite was not detected, as might be expected from the alteration of clarkeite. The Na in clarkeite was evidently lost to ground water during the alteration to uranophane. The fate of Th, Y, and REE is uncertain; these elements were not detected in the uranophane by EMP analysis. Thus, Th and Y may have precipitated as insoluble minerals (e.g., $ThSiO_4$ or YPO_4) and occur as inclusions within the uranophane, or these elements may have been adsorbed onto other minerals. The REEs may have been transported as soluble carbonate complexes.

Acknowledgments

This research was supported by the Swedish Nuclear Fuel and Waste Management Co. (SKB). The authors are indebted to C. Francis (Harvard University Mineralogy Museum), G. Mast (Colorado School of Mines Geology Museum) and J. Murphy (Denver Museum of Natural History) for the clarkeite samples. We are grateful to C.J. Yapp for his advice on reactions and thermodynamics and to M.L. Miller for his assistance with XRD and for many fruitful discussions about crystal chemistry. We are also grateful to T. Ledford, G. Ledford, and B. Mattison for helpful information about the Spruce Pine area. XRD data were collected at the X-ray Diffraction Laboratory in the Department of Earth and Planetary Sciences, University of New Mexico, and at the Department of Geological Sciences at the University of Manitoba. Computing facilities for Rietveld refinement were made available by F.C. Hawthorne, Department of Geological Sciences, University of Manitoba. Electron microprobe analyses were performed at the Electron Microbeam Analysis Facility at the Department of Earth and Planetary Sciences, University of New Mexico. The manuscript benefited from careful reviews by S. Simmons, J. Jambor, and A. Falster.

References cited

Albee, A.L. and Ray, L. (1970) Correction factors for electron microanalysis of silicates, oxides, carbonates, phosphates and sulfates. Analytical Chemistry, 42, 1408–1414.

Bence, A.E. and Albee, A.L. (1968) Empirical correction factors for the electron microanalysis of silicates and oxides. Journal of Geology, 76, 382–403.

Bobo, J.-C. (1964) Contribution à la connaisance physique et chimique des systèmes formés par l'uranium, l'oxygène et un élément métallique. Revue de Chimie Minérale, 1, 1–37.

Brisi, C. and Appendino, M.M. (1969) Ricerche sugli uranati di calcio. Annali di Chimica (Rome), 59, 400–411.

Brown, I.D. (1981) The bond-valence method: An empirical approach to chemical structure and bonding. In M. O'Keefe and A. Navrotsky, Eds., Structure and Bonding in Crystals II, p. 1–30. Academic Press, New York.

Bruno, J., Casas, I., Cera, E., Ewing, R.C., Finch, R.J., and Werme, L.O. (1995) The assessment of the long-term evolution of the spent nuclear fuel matrix by kinetic, thermodynamic and spectroscopic studies of uranium minerals. Materials Research Society Proceedings, 353, 633–639.

Burns, P.C., Miller, M.L., and Ewing, R.C. (1996) U^{6+} minerals and inorganic phases: a comparison and hierarchy of crystal structures. Canadian Mineralogist, 34, 845–880.

Čejka, J. (1969) To the chemistry of andersonite and thermal decomposition of dioxotricarbonatouranates. Collection, Czechoslovakia Chemistry Communications, 34, 1635–1657.

Čejka, J. and Urbanec, Z. (1990) Secondary Uranium Minerals. (Academia, Czechoslovak Academy of Sciences, Prague) 93 p.

Cordfunke, E.H.P. and Loopstra, B.O. (1971) Sodium uranates: preparation and thermochemical properties. Journal of Inorganic and Nuclear Chemistry, 33, 2427–2436.

Deliens, M. (1977) Review of the hydrated oxides of U and Pb, with new X-ray powder data. Mineralogical Magazine, 41, 51–57.

Evans, H.T. (1963) Uranyl ion coordination. Science, 141, 154–158.

Ewing, R.C. (1993) The long-term performance of nuclear waste forms: Natural materials—three case studies. Materials Research Society Proceedings, 294, 559–568.

Finch, R.J. and Ewing, R.C. (1991) Uraninite alteration in an oxidizing environment and its relevance to the disposal of spent nuclear fuel. SKB Technical Report 91-15 (Swedish Nuclear Fuel and Waste Management Co., Stockholm) 114 p.

——— (1992) The corrosion of uraninite under oxidizing conditions. Journal of Nuclear Materials, 190, 133–156.

——— (1993) The alteration of uraninite to clarkeite. Materials Research Society Proceedings, 294, 513–520.

Finch, R.J., Cooper, M.A., Hawthorne, F.C., and Ewing, R.C. (1996a) The crystal structure of schoepite, $[(UO_2)_8O_2(OH)_{12}](H_2O)_{12}$. Canadian Mineralogist, 34, 1071–1088.

Finch, R.J., Hawthorne, F.C., and Ewing, R.C. (1996b) Schoepite and dehydrated schoepite. In: Scientific Basis for Nuclear Waste Management XIX (W.M. Murphy and D.A. Knecht, editors) Materials Research Society Proceedings, 412 (MRS, Pittsburgh) 831–838.

Fonteneau, G., L'Helgoualch, H., and Lucas, J. (1975) Les uranates de sodium et la lanthanides. Revue de Chimie Minérale, 12, 382–390.

Frondel, C. (1956) The mineral composition of gummite. American Mineralogist, 41, 539–568.

——— (1958) Systematic Mineralogy of Uranium and Thorium. US Geological Society Bulletin, 1064, 400 p.

Frondel, C. and Meyrowitz, R. (1956) Studies of uranium minerals (XIX): rutherfordine, diderichite and clarkeite. American Mineralogist, 41, 127–133.

Gruner, J. (1954) The chemical formula of clarkeite. American Mineralogist, 39, 836–838.

Janecek, J. and Ewing, R.C. (1992) Dissolution and alteration of uraninite under reducing conditions. Journal of Nuclear Materials, 190, 157–173.

Kovba, L.M., Ippolitova, E.A., Simanov, Yu.P., and Spitsyn, V.I. (1958) X-ray diffraction investigation of alkali metal uranates. Doklady Akademii Nauk SSSR, 120, 1042–1044. (in Russian)

Kovba, L.M., Simanov, Yu.P., Ippolitova, E.A., and Spitsyn, V.I. (1961) On the crystalline structure of diuranates of alkali elements. In V.I.

Spitsyn, Ed., Issledovaniya v oblasti khimii urana, p. 21–28. Moscow University Press, Moscow (in Russian). (English translation: Argonne National Laboratory translation series, ANL-trans-33, from CFSTI.)

Lindemer, T.B., Besmann, T.M., and Johnson, C.E. (1981) Thermodynamic review and calculations—alkali-metal oxide systems with nuclear fuels, fission products, and structural materials. Journal of Nuclear Materials, 100, 178–226.

Loopstra, B.O. (1970a) The structure of β-U_3O_8. Acta Crystallographica, B26, 656–657.

———(1970b) The phase transition in α-U_3O_8 at 210 °C. Journal of Applied Crystallography, 3, 94–96.

Loopstra, B.O. and Rietveld, H.M. (1969) The crystal structures of some alkaline-earth uranates. Acta Crystallographica, B25, 787–791.

Mereiter, K. (1979) The crystal structure of curite, $[Pb_{6.56}(H_2O,OH)_4][(UO_2)_8O_6(OH)_8]_2$. Tschermaks Mineralogische und Petrologische Mitteilungen, 26, 279–292.

Pagoaga, M.K., Appleman, D.E., and Stewart, J.M. (1987) Crystal structure and crystal chemistry of the uranyl oxide hydrates becquerelite, billietite, and protasite. American Mineralogist, 72, 1230–1238.

Piret, P. (1985) Structure cristalline de la fourmariérite, $Pb(UO_2)_4O_3(OH)_4 \cdot 4H_2O$. Bulletin de Minéralogie, 108, 659–665.

Piret, P., Deliens, M., Piret-Meunier, J., and Germain, G. (1983) La sayrite, $Pb_2[(UO_2)_5O_6(OH)_2] \cdot 4H_2O$, nouveau minéral; propriétés et structure cristalline. Bulletin de Minéralogie, 106, 299–304.

Piret-Meunier, J. and Piret, P. (1982) Nouvelle détermination de la structure cristalline de la becquerelite. Bulletin de Minéralogie, 105, 606–610.

Rietveld, H.M. (1969) A profile refinement method for nuclear and magnetic structures. Journal of Applied Crystallography, 2, 65–71.

Rogova, V.P., Belova, L.N., Kiziyrov, G.P., and Kuznetsova, N.N. (1974) Calciouranoite, a new hydroxide of uranium. Zapiski Vsesoyuznogo Mineralogicheskogo Obshchestva, 103, 103–109 (In Russian). (English abstract: American Mineralogist, 60, 161.)

Ross, C.S., Henderson, E.P., and Posnjak, E. (1931) Clarkeite, a new uranium mineral. American Mineralogist, 16, 213–220.

Smith, D.K., Jr. (1984) Uranium mineralogy. In B. DeVivo, F. Ippolito, G. Capaldi and P.R. Simpson, Eds., Uranium Geochemistry, Mineralogy, Geology, Exploration and Resources, p. 43–88. Institute of Mining and Metallurgy, London.

Stohl, F. and Smith, D.K. (1981) The crystal chemistry of the uranyl silicate minerals. American Mineralogist, 66, 610–625.

Taylor, J.C. (1971) The structure of the α form of uranyl hydroxide. Acta Crystallographica, B27, 1088–1091.

Toussaint, C.J. and Avogadro, A. (1974) Concerning uranate formation in alkali nitrate melts. Journal of Inorganic and Nuclear Chemistry, 36, 781–784.

Vochten, R., Blaton, N., Peeters, O., Van Haverbeke, L., and Van Springel, K. (1997) Synthesis of boltwoodite, its transformation into sodium boltwoodite and the physicochemical characteristics of boltwoodites. Canadian Mineralogist (in press).

Wamser, C.A., Belle, J., Bernsohn, E., and Williamson, B. (1952) The constitution of the uranates of sodium. Journal of the American Chemical Society, 74, 1020–1022.

Wiles, D.B. and Young, J. (1981) A new computer program for Rietveld analysis of X-ray powder diffraction patterns. Journal of Applied Crystallography, 14, 149–151.

Manuscript received October 21, 1996
Manuscript accepted February 3, 1997